



OPEN

Radical pair model for magnetic field effects on NMDA receptor activity

Parvathy S. Nair¹✉, Hadi Zadeh-Haghighi^{2,3,4}✉ & Christoph Simon^{2,3,4}✉

The *N*-methyl-D-aspartate receptor is a prominent player in brain development and functioning. Perturbations to its functioning through external stimuli like magnetic fields can potentially affect the brain in numerous ways. Various studies have shown that magnetic fields of varying strengths affect these receptors. We propose that the radical pair mechanism, a quantum mechanical process, could explain some of these field effects. Radicals of the form $[\text{RO}^{\cdot}\text{Mg}(\text{H}_2\text{O})_n^+]$, where R is a protein residue that can be Serine or Tyrosine, are considered for this study. The variation in the singlet fractional yield of the radical pairs, as a function of magnetic field strength, is calculated to understand how the magnetic field affects the products of the radical pair reactions. Based on the results, the radical pair mechanism is a likely candidate for explaining the magnetic field effects observed on the receptor activity. The model predicts changes in the behaviour of the system as magnetic field strength is varied and also predicts certain isotope effects. The results further suggest that similar effects on radical pairs could be a plausible explanation for various magnetic field effects within the brain.

Magnetic field effects (MFEs) in biological systems have garnered considerable attention from the academic community. This has been studied in the context of numerous systems, such as magnetoreception¹, the working of the circadian clock², genetics³, and various others^{4–15}. In the last few decades, there has been significant progress in modelling different MFEs in these systems based on quantum mechanical phenomena¹⁶. One model that has been quite promising in explaining some of these effects is the radical pair mechanism (RPM)¹⁷. This mechanism explains the behavior of radical pair electrons, which are pairs of correlated electrons formed on separate molecules from the rupture of chemical bonds or through electron hopping. The RPM model has been most commonly applied in explaining avian magnetoreception in migratory birds¹⁸. It has also been used to model magnetoreception in other migratory organisms¹⁹, as well.

There are numerous phenomena involving MFEs in biological systems that have yet to be explained by any mechanisms. One of the most fascinating areas to study such phenomena is the brain. It has been found that exposure to magnetic fields affects various functions in the brain. The frequency of neuron firing, pain sensitivity and inhibition, production of melatonin, and functioning of the pineal gland are some examples of these effects⁶.

Understanding the effects of magnetic fields on the brain is especially important since magnetic stimulations are already a well-known and well-used method for non-invasive brain stimulation used as both diagnostic and therapeutic tools^{20–22}. Since magnetic stimulations can modulate various brain functions, they also have the potential to be used as a treatment for numerous neuropsychiatric diseases^{23,24}. Understanding the mechanism by which magnetic fields affect important parts of the brain could potentially lead to further advances in such non-invasive treatment tools.

Despite the existence of a large number of studies on these phenomena, there still needs to be more understanding of the mechanisms by which most of these effects occur. However, the RPM model has recently been applied to studying various phenomena within the brain with promising results. According to this mechanism, the electrons on the RP involved evolve under the influence of various interactions, like the Zeeman and hyperfine interactions, into a superposition of singlet and triplet states. The rate and yield of the final products formed from these states are affected by external magnetic fields, which is the cause of the various experimental observations. Lithium effects on hyperactivity²⁵, magnetic field and lithium effects on the working of the circadian clock²⁶, hypomagnetic field effects on neurogenesis²⁷, hypomagnetic field effects on microtubule reorganization²⁸, and

¹Department of Physics, Indian Institute of Science Education and Research (IISER), Tirupati, Tirupati, Andhra Pradesh 517507, India. ²Department of Physics and Astronomy, University of Calgary, Calgary, AB T2N 1N4, Canada. ³Institute for Quantum Science and Technology, University of Calgary, Calgary, AB T2N 1N4, Canada. ⁴Hotchkiss Brain Institute, University of Calgary, Calgary, AB T2N 1N4, Canada. ✉email: parvathysnair@students.iisertirupati.ac.in; hadi.zadehaghighi@ucalgary.ca; csimo@ucalgary.ca

Xenon-induced general anesthesia²⁹ are examples of the various phenomena that have been modelled using this mechanism. These results encourage us to apply the mechanism to understand other phenomena within the brain.

One of the examples of such phenomena is the MFEs on the functioning of the *N*-Methyl-D-Aspartate receptors (NMDARs) within the brain. Several experimental studies successfully show that both static and oscillating magnetic fields of different strengths can affect the activity of NMDARs^{30,31}. These receptors are critical in all stages of development in higher organisms and are heavily involved in various brain functions, such as neuronal development and synaptic plasticity³². The wide range of roles this receptor plays in the brain makes it a rich subject for research, with numerous studies dedicated to understanding its structure, function, and physiological roles over the years^{33,34}. The variations in the different subunits that form this receptor increase the complexity and functionality of the various forms of the receptor^{35,36}. As these receptors are deeply involved in the development and functioning of the brain, they are also crucial players in numerous neurological and psychological disorders. NMDARs have been shown to be involved in ischemic strokes, schizophrenia, excitotoxic brain injury, memory and learning impairments, and various other disorders^{37–40}, thus making it extremely important that we understand the effects of external MFEs on these receptors and how they affect different processes within the brain.

Hirai et al. demonstrated in two separate studies^{41,42} that immature rat hippocampal cells cultured in the presence of a 100 mT sustained or repetitive static magnetic field exhibit an increase in intracellular free Ca^{2+} ion concentration upon increasing NMDA concentration. In both experiments, upregulation of certain mRNAs that encode some of the NMDAR subunits was observed.

We propose that an RPM model could provide an explanation for the observed effects. The MFE observed in these experiments may be occurring at any level, ranging from the transcription of the NMDAR subunits mRNAs to a direct effect on the functioning of the receptor. We attempt to identify the possible radical pairs involved in the various reaction pathways in these levels that may be affected by the static magnetic field (SMF). The potential RPs are identified based on the experimental evidence presented previously and an understanding of the mechanisms involved in the formation and function of the NMDAR. We study the effects of the magnetic field by calculating the product yield of the possible radical pair reactions involved in the system. On the basis of our findings, we conclude that an RPM model could provide a plausible explanation for the magnetic field effects observed on the NMDAR activity. This also provides further indication that radical pairs could be a key player in various magnetic field effects that occur in the brain. We further predict variations in the behaviour of the system as the magnetic field strength varies, which could be experimentally studied. We also show that there may be certain isotope-dependent effects that could also be of experimental interest.

Results

Results from previous experiments

Hirai et al.⁴¹ conducted an experiment in which immature rat hippocampal cells were cultured for three days in vitro (DIV) in the presence of 100 mT SMF. Following the exposure, an increase in the intake of Ca^{2+} ions was observed as the NMDA concentration within the cells was increased. In addition, an upregulation in the expression of mRNA encoding the NR1, NR2A-D, and NR3A subunits of NMDAR was observed in these cells following exposure.

In a separate study conducted by Hirai et al.⁴², immature rat hippocampal cells were repeatedly exposed to 100 mT SMF for 15 min per day for 8 days. Upon harvesting the cells 24 h after the final exposure, it was found that there was once again a significant increase in intracellular Ca^{2+} ion concentration. An upregulation in the mRNA expression of just the NR2B subunit of NMDAR by a factor of ~ 1.4 was also reported under the effect of such an exposure.

Tables 1 and 2 contain data from the experiments conducted by Hirai et al. The data is approximate and has been extracted from plots in the two papers that visualize the variation of Ca^{2+} ion concentration in the presence of the SMF, as NMDA concentration is varied.

From the same experiments, Hirai et al. also reported an increase in the binding activity of Activator Protein-1 (AP-1), which is a transcription factor that has been shown to be an active regulator of NR2B transcription⁴³.

NMDA concentration (μM)	Cytoplasmic Ca^{2+} conc. in control setup (%)	Cytoplasmic Ca^{2+} conc. at 100 mT (%)	Ratio of conc. at 100 mT vs. control setup
1	6.2	11.5	1.8
3	15.1	23.7	1.6
10	21.1	30.6	1.4
30	24.7	33.2	1.3
100	26.9	33.7	1.2

Table 1. Approximate quantification of the experimental observations reported by Hirai et al.⁴¹ of sustained exposure to SMF on the extent of Ca^{2+} intake into rat hippocampal cells. Immature rat hippocampal cells were cultured for three days in vitro (DIV) in the presence of 100 mT SMF for this experiment. The values in the table are expressed as percentages over the maximal reading found at the end of the experiments from an addition of 10 μM of Ca^{2+} ionophore (A23187).

NMDA concentration (μM)	Cytoplasmic Ca^{2+} in control setup (%)	Cytoplasmic Ca^{2+} at 100 mT (%)	Ratio of Ca^{2+} at 100 mT vs. control setup
1	3.9	6.2	1.6
3	10.2	16.3	1.6
10	17.9	25.8	1.4
30	22.8	28.2	1.2
100	25.1	28.4	1.1

Table 2. Approximate quantification of the experimental observations reported by Hirai et al.⁴² of repeated exposure to SMF on the extend of Ca^{2+} intake into rat hippocampal cells. Immature rat hippocampal cells were repeatedly exposed to 100 mT SMF for 15 min per day for 8 days for this experiment. The values in the table are expressed as percentages over the maximal reading found at the end of the experiments from an addition of 10 μM of Ca^{2+} ionophore (A23187).

Possible role of phosphorylation in MFE on NMDARs

The first possible explanation for the MFE is an increase in NMDAR activity as a result of a rise in the number of mRNAs that form these receptors. Prybylowski et al.⁴⁴ demonstrated that an increase in the number of NR2 subunits within cerebellar granule cells causes an increase in the concentration of NMDARs within the cells. The same is most likely true for hippocampal cells.

As stated previously, an increase in the NR2B mRNA concentration is observed within the cells in the presence of an SMF^{41,42}. It is highly likely that an increase in mRNA concentration would also result in an increase in NR2B subunit concentration within the cells. According to the findings of Prybylowski et al., the increase in NR2B subunits should result in an increase in the number of NMDARs in the cell. An increase in the number of NMDARs provides more channels for the Ca^{2+} ions to enter the cells, thus causing an increase in the concentration of these ions within the cells, as the concentration of NMDA in the culture increases.

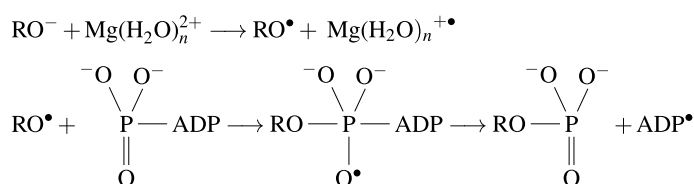
The upregulation in NR2B mRNA expression observed in the experiments could have occurred as the result of an MFE occurring at any stage of the mRNA formation. The increase in AP-1 binding activity reported by Hirai et al. could be a possible explanation for the same. AP-1 transcription factors typically consist of heterodimers of Jun and Fos proteins or homodimers of Jun proteins. The DNA binding activity of AP-1 is regulated by phosphorylation and dephosphorylation processes of the c-Jun protein, which belongs to the Jun protein family. Phosphorylation of Ser 63 and Ser 73 in the N-terminal domain of c-Jun stimulates the transcriptional activity of the protein^{45,46}. Phosphorylation has been reported to be affected by MFEs^{47–49}, making this process a likely candidate for the SMF effects.

As mentioned previously, it is also possible that the MFE occurs directly on the NMDAR or its subunits. Phosphorylation of serine and tyrosine sites in NMDAR subunits has been shown to regulate NMDAR activity^{50,51}. For instance, phosphorylation of Ser 896 and Ser 897 together increases NMDAR surface expression. Receptor currents increase in NMDARs containing NR2A subunits when Ser 1291 and Ser 1312 are phosphorylated. Tyrosine phosphorylation of NR2A also potentiates NMDAR currents. These phosphorylation processes can also be influenced by MFEs.

We propose that the MFEs reported on NMDAR activity may be modeled by an RPM model based on the effects of SMF on one of the aforementioned processes. The MFE could occur via either a Serine phosphorylation, which will be referred to as the “Ser Pathway”, or a tyrosine phosphorylation, which will be referred to as the “Tyr Pathway”.

RPM model of oxyradicals and hydrated magnesium cations

Buchachenko et al.⁵² theorized that the transfer of phosphate groups to proteins induced by protein kinases may involve an ion-radical mechanism. They studied the catalysis of phosphorylation of prothrombin by prothrombin kinases with $^{24}\text{Mg}^{2+}$ and $^{25}\text{Mg}^{2+}$ ions, where they successfully demonstrated an isotope dependence in the kinase's efficiency, which could be due to the nuclear spin of the Mg^{2+} isotopes. It was proposed that this indicates that the ion-radical mechanism could be a plausible mechanism for enzymatic phosphorylation processes. The mechanism involves the following reactions:



According to this mechanism, phosphorylation could involve an oxyradical, RO^\bullet (where R represents a protein residue), and a hydrated magnesium cation radical, $\text{Mg}(\text{H}_2\text{O})_n^{+\bullet}$.

Depending on the pathway involved, the protein residue for our system could be either Serine or Tyrosine. Based on this, we propose that the MFEs can be modeled by an RPM model involving the RP [$\text{RO}^\bullet \text{Mg}(\text{H}_2\text{O})_n^{+\bullet}$]

formed during this reaction. The reactions involved in the transcriptional level phosphorylation processes involve only the Ser Pathway, whereas the Ser or Tyr Pathways may be involved in the MFEs on NMDAR subunits.

We model the MFEs on the RPs using a simplified Hamiltonian consisting only of Zeeman and hyperfine interactions (HFIs), which is a good approximation for sufficiently distant radicals^{18,53}. We assume that radical electrons have the same *g*-value as free electrons, which is a good approximation at the field values we are interested in. We also consider only the isotropic Fermi contact contribution for the HFIs, as the molecular arrangement is likely to be random. Therefore, the Hamiltonian would have the following form:

$$\hat{H} = \omega(\hat{S}_{A_z} + \hat{S}_{B_z}) + a_A \hat{S}_A \cdot \hat{I}_A + a_B \hat{S}_B \cdot \hat{I}_B.$$

Here, \hat{S}_A and \hat{S}_B are the electron spin operators of the RPs labelled *A* and *B*, respectively. The Larmor frequency of the electrons due to Zeeman interaction is given by ω . \hat{I}_A represents the nuclear spin operator associated with the oxyradical nucleus that contributes most to the HFI.

We perform our calculations considering the contributions from the natural abundance of the different magnesium isotopes. It is well known that 10% of naturally occurring magnesium is composed of the isotope ²⁵Mg, which is a spinful isotope (with spin 5/2). In the equation above, \hat{I}_B represents the nuclear spin operator of any naturally occurring ²⁵Mg nucleus present in the system. The terms a_A and a_B are the hyperfine coupling constants for each of the nuclei.

We use density functional theory (DFT) calculations to determine the hyperfine coupling constant (HFCC) values for all spinful nuclei involved. The details for the same have been given in the “Methods” section. For our calculations, we consider the HFI contribution from only the nucleus with the highest HFCC, which is a commonly used approximation. In the case of the Serine oxyradical, we find that the highest HF contribution is from a hydrogen nucleus with $a_A = 7.45$ mT. For the Tyrosine oxyradical, the highest HFCC is of one of the hydrogen nuclei with $a_{A_1} = 1.86$ mT. The HFCC of the ²⁵Mg isotope is $a_B = -11.22$ mT.

Singlet yield calculations

The fractional singlet yield of the reaction with and without the magnetic field indicates how the SMF affects the rate of formation of the different reaction products. This could lead to further changes in the reaction rates or product concentrations of various reactions involved in the pathways leading to the experimentally observed effects²⁶.

The fractional yield of a reaction is calculated by tracking the spin state of the RP during the reaction. This calculation can be carried out by solving the Liouville-von Neumann equation, which describes the evolution of the density matrix over time¹⁷. For a general singlet-born RP under the effect of a weak magnetic field, the fractional yield for periods larger than the lifetime of the RPs is found from the eigenvalues and eigenvectors of the Hamiltonian as:

$$\Phi_S = \frac{1}{M} \sum_{m=1}^{4M} \sum_{n=1}^{4M} |\langle m | \hat{P}^S | n \rangle|^2 \frac{k(k+r)}{(k+r)^2 + (\omega_m - \omega_n)^2} - \frac{k}{4(k+r)} + \frac{1}{4},$$

where $M = M_A M_B$, $M_X = \prod_i^{N_X} I_{iX}(I_{iX} + 1)$ is the nuclear spin multiplicity, $|m\rangle$ and $|n\rangle$ are the eigenstates of the hamiltonian, \hat{H} , with the eigenenergies given by ω_m and ω_n , respectively, and \hat{P}^S is the singlet projection operator acting on the electron spins. Here, we assume that the singlet and triplet reaction rates are equal and are denoted by k . Finally, r is the relaxation rate or spin-coherence lifetime of the radical pairs⁵⁴. The above equation is an approximation based on the fact that the spin-lattice and spin-spin relaxation times of the system would be approximately equal when the magnetic field strength is close to zero. Further calculations considering different relaxation times are available in the Supplementary Material.

As mentioned above, Φ_S provides information about the yield of the different reaction products with and without the effect of the SMF. We connect this change in the yield of the products to the change in the intracellular concentration of Ca²⁺ ions, in order to understand the MFE on the cells.

Due to the lack of experimental data for the exact values of the reaction rate, k , and relaxation rate, r , of the RP we consider, we explore the k/r space for an approximate range of potential values. We consider the ratio of Φ_S at 100 mT (B_{exp}), which is the experimental field strength considered by Hirai et al.^{41,42}, to Φ_S at the control magnetic field strength (B_0):

$$S = \frac{\Phi_S \text{ at } B_{\text{exp}}}{\Phi_S \text{ at } B_0}.$$

We plot this quantity against a range of possible k and r values. The magnitude of the ratio reflects the extent of the magnetic field effects on radical pair electrons, which we compare to the magnitude of the ratio of Ca²⁺ concentrations within the cells, as shown in Tables 1 and 2.

Ser pathway

Figure 1a depicts a plot of S versus k and r for the radical pair containing the serine oxyradical. In this calculation, we consider the contribution of all Magnesium isotopes according to their natural abundance. As the magnetic field strength for the control setup of the experiment conducted by Hirai et al.^{41,42} ranged from $B_0 = 0-0.3$ mT, we take $B_0 = 0.15$ mT as our control value. Here, the lighter yellow colored areas of the plot within the black outline represent the values of k and r for which there is the greatest variation in Φ_S between B_0 and B_{exp} . These points have the potential to capture the behaviour of the system, as they match the magnitude of the ratio of

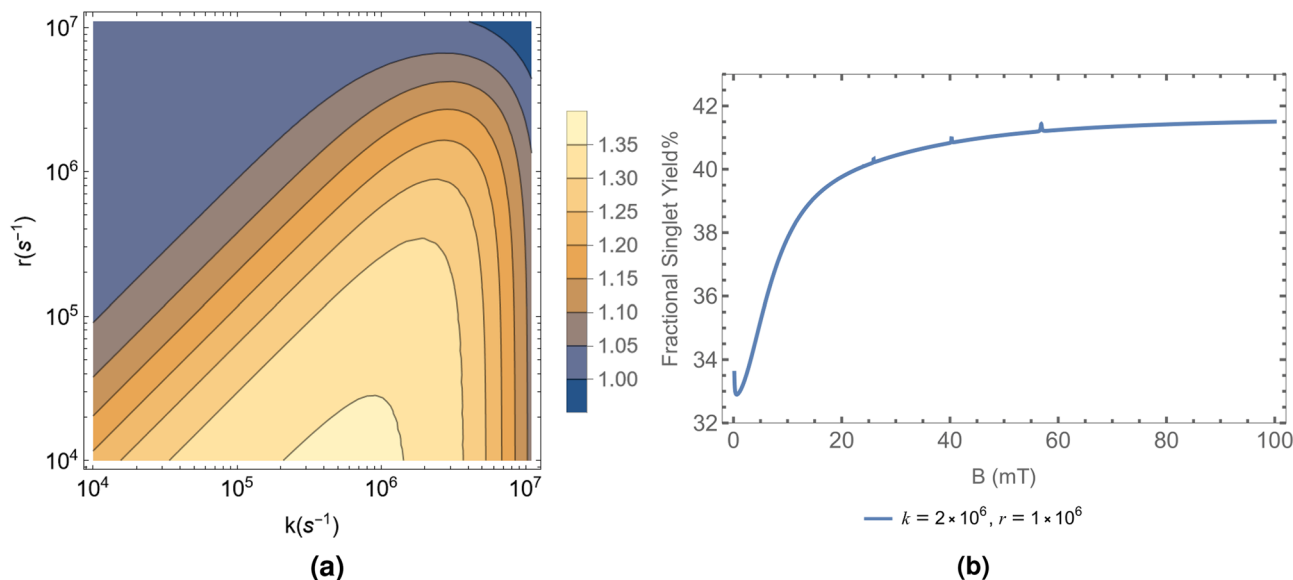


Figure 1. (a) Ratio of Φ_S percentages, S plotted in the $k - r$ plane for the Ser Oxyradical case. The lighter yellow areas are closest in value to the ratios seen in Tables 1 and 2. (b) Variation of Φ_S percentage with magnetic field strength ranging from 0.15 to 100 mT. The figure is plotted with $k = 2 \times 10^6 \text{ s}^{-1}$ and $r = 1 \times 10^6 \text{ s}^{-1}$, which corresponds to $S = 1.24$. All the figures are plotted considering the HFI contribution from the hydrogen atom of the Serine oxyradical with the highest HFCC, $a_A = 7.45 \text{ mT}$. We also consider the contribution of the ^{25}Mg isotope at its natural abundance of 10%. The HFI contribution from the same is $a_B = -11.22 \text{ mT}$.

Ca^{2+} concentration in the control vs. experimental setups. The values of k and r are consistent with typical values considered in the literature on the RPM.

Examples of the variation of Φ_S percentage with magnetic field strength from 0.15 to 100 mT for two different choices of k and r from the feasible range of values are given in Fig. 1.

Tyr pathway

Similar to what we have done for the case of the Ser Pathway, the quantity S was calculated and plotted against physically feasible ranges of k and r for the radical pair involving the tyrosine oxyradical. Figure 2a shows the same.

Figure 2 also shows examples of the variation of Φ_S percentage with magnetic field strength from 0.15 to 100 mT for two different values of k and r .

In these calculations, Φ_S was found to exhibit a few spikes at certain values of the MF strength, B , for both the Ser and Tyr pathways. These spikes are associated with certain eigenstates overlapping in energy due to the effect of the spin of the ^{25}Mg isotope. More results regarding the contribution from the individual isotopes are presented in Supplementary Information.

A dip in Φ_S values at very weak B is also seen in Figs. 1b and 2b. This occurs due to the low field effect¹⁷. The extent of the drop in Φ_S from the value at B_0 increases as k increases for both Ser and Tyr Pathways. However, there is no significant difference in the drop of Φ_S from the value at $B = 0$ for either pathway.

Discussion

The primary objective of this study was to determine whether the radical pair mechanism can provide a plausible explanation for the magnetic field effects on NMDAR activity reported by Hirai et al.^{41,42}. We find that a simple RP model is capable of capturing the MFEs on the system, as the magnitude of the MFE on the singlet yield corresponds well to the magnitude of the experimental MFE observed on the Ca^{2+} ion concentration within the cells. It has been shown above that both Serine and Tyrosine phosphorylation could be involved in the upregulation of NMDAR activity in the presence of a static magnetic field. Serine phosphorylation is involved in activating the AP1 transcription factor, which is a major regulator of the NR2B subunit. As described previously, an increase in NR2B can increase the number of NMDARs in the system, resulting in an increase in the calcium ion influx into the cells. We have also seen how phosphorylation of certain NMDAR Subunits at Serine and Tyrosine sites may also cause an increase in NMDAR activity, which again raises the possibility that magnetic field effects occur through the phosphorylation processes. We thus propose that the radical pairs involved in the ion-radical mechanism of phosphorylation could be a likely candidate for the RPM model. We thus consider radical pairs of the form $[\text{RO} \cdot \text{Mg}(\text{H}_2\text{O})_n^+]$, where the protein residue, R could be a Tyrosine or Serine residue. The Mg(I) radical species has not yet been experimentally observed in biological systems. However, there is evidence for the existence of stable Mg(I) organic compounds⁵⁵. Various research studies also show magnetic isotope effects with magnesium ions, and also with other ions, that could most likely be explained by the ion radical mechanism⁵⁶⁻⁶⁶.

It bears mentioning that Crotty et al.⁶⁷ made an attempt to reproduce one of the magnetic isotope effects reported by Buchachenko's group, but their experiment did not find any significant results. This does not

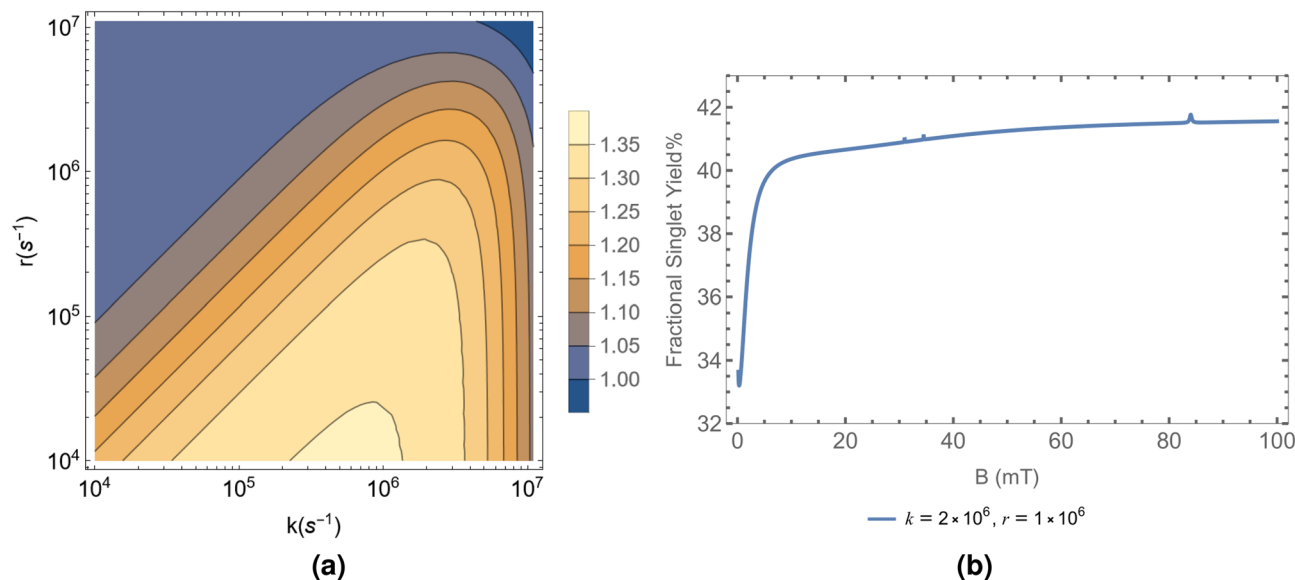


Figure 2. (a) Ratio of Φ_S percentages, S , plotted in the $k - r$ plane. The lighter yellow areas are closer in value to the ratios seen in Tables 1 and 2. (b) Variation of Φ_S percentage with magnetic field strength ranging from 0.15 to 100 mT. The figure is plotted with $k = 2 \times 10^6 \text{ s}^{-1}$ and $r = 1 \times 10^6 \text{ s}^{-1}$, which corresponds to $S = 1.24$. All the figures are plotted considering the HFI contribution from the hydrogen atom of the Tyrosine oxyradical with the highest HFCC, $a_A = 1.86 \text{ mT}$. We also consider the contribution of the ^{25}Mg isotope at its natural abundance of 10%. The HFI contribution from the same is $a_B = -11.22 \text{ mT}$.

necessarily mean that the original results are incorrect, as reproducibility in biology is a challenge both in the case of low magnetic field effects^{6,16,54,68,69} and in general⁷⁰, likely due to the complexity of biological systems⁷¹. Further, the numerous studies mentioned earlier that report magnetic isotope effects with Mg and other ions also suggest that there is a good possibility for these effects to be significant.

Based on the experimental evidence found by Hirai et al., there is an increase in the concentration of Ca^{2+} ions within the hippocampal cells in the presence of magnetic fields. For cells exposed to a sustained or repetitive SMF, an increase in concentration of the ions by an average factor of about 1.5 and 1.4, respectively, has been observed. So far, our results indicate that this variation in the behavior of the system in the presence of the magnetic field could indeed be explained using an RPM model.

The radical pairs involving both the Serine and Tyrosine pathway models exhibit significant variation in singlet yield percentage in the presence of the magnetic field. We find that both models capture a variation in Φ_S by a factor of 1.24 in the presence of the 100 mT magnetic field for certain plausible values of k and r . Based on these results, we propose that the increase in the yield of the singlet product of the reaction could be leading to the increase in the Ca^{2+} ion concentration through various biochemical reactions within the system. Though the increase of the singlet yield of the model is not exactly equal to the experimentally observed increase in the Ca^{2+} concentration, it is plausible that an amplification of the effects could occur through the various processes involved in the Ca^{2+} ion intake into the cells. Multiple studies have shown that such amplifications are a promising possibility in numerous systems involving the RPM model^{72–75}. Therefore, we propose that both the Ser and Tyr Pathways could potentially explain the MFE observed in experiments. However, there is limited evidence of the formation of serine radicals, particularly in biological systems^{76–78}.

It is worth noting that the radical pairs under consideration could be involved in various other reactions within the biological system, which could also play a role in the variations in activity seen in the experiments by Hirai^{41,42}. Furthermore, as can be seen from the results, the variation in the magnetic field effects seen between the Tyrosine and Serine radicals is fairly low, which could mean that other radical pairs involved in various reactions related to NMDAR activity could also be involved in the observed MFE. It is also worth noting that the contribution from the ^{25}Mg isotope does not impact the results very significantly as we only consider the contributions based on the natural abundance of the isotopes, of which ^{25}Mg is only 10%.

Based on the results we have presented, we propose that the radical pair mechanism is a promising model to explain the effects of the magnetic field effects on NMDAR activity. While the model involving Serine/Tyrosine radicals and Mg(I) radicals could be a possible example of how the system works, RPM mechanisms involving other radical pairs could also be the cause of the observed behaviour. New experiments studying the effect of magnetic field strength on NMDA activity could give further insight into the behaviour of the system and the accuracy of the results from our model. Further experiments could also be conducted to study the likelihood of Serine and Tyrosine radical formation in the system and the role they could play in the pathways leading to the MFE on NMDA activity. The most common method for radical detection in biological systems is EPR spectroscopy. Direct EPR spectroscopy could be used to detect the presence of the Tyrosine radicals as they are long-lived due to stabilization by electron delocalization. There is some evidence of EPR and time-resolved EPR being successfully used to study Serine radicals^{76,78}. These could potentially be used to study if these radicals are present in a given system. Experiments that study the effects of the magnetic field in a system with a higher

concentration of the ^{25}Mg isotope could also be interesting, as we find certain isotope-dependent effects in the calculation of Φ_S , which is discussed in detail in Supplementary Information.

It is possible that similar models based on the RPM could be used to understand magnetic field effects on various other biological processes. Furthering our understanding of how external stimuli like magnetic fields affect the different processes within the brain could lead to a much deeper understanding of its working. It could also provide significant insights into finding ways to diagnose and treat various neuropsychiatric and psychological disorders, as well, thus making this simultaneously an intriguing and practically relevant field of study.

Methods

DFT analysis

The DFT calculations for our radical pairs were performed using the ORCA package⁷⁹. The optimization of the molecular structures was performed using the dispersion-corrected PBE0 functional and the def2-TZVP basis set.

The hyperfine coupling constants were calculated from the orbitals obtained from the optimization calculations. The B3LYP functional and def2-TZVP basis set were used for the calculation of both the HFCCs, a_A , and a_B . The solvent effects in every calculation were considered using the conductor-like polarizable continuum model (CPCM) with a dielectric constant of 2.

Data availability

The generated datasets and computational analysis are available from the corresponding author upon reasonable request.

Received: 25 October 2023; Accepted: 12 February 2024

Published online: 13 February 2024

References

- Johnsen, S. & Lohmann, K. J. The physics and neurobiology of magnetoreception. *Nat. Rev. Neurosci.* **6**, 703–712. <https://doi.org/10.1038/nrn1745> (2005).
- Lewczuk, B. *et al.* Influence of electric, magnetic, and electromagnetic fields on the circadian system: Current stage of knowledge. *Biomed. Res. Int.* **2014**, 1–13. <https://doi.org/10.1155/2014/169459> (2014).
- McCann, J., Dietrich, F. & Rafferty, C. The genotoxic potential of electric and magnetic fields: An update. *Mutat. Res. Rev. Mutat. Res.* **411**, 45–86. [https://doi.org/10.1016/s1383-5742\(98\)00006-4](https://doi.org/10.1016/s1383-5742(98)00006-4) (1998).
- Ketchen, E., Porter, W. & Bolton, N. The biological effects of magnetic fields on man. *Am. Ind. Hyg. Assoc. J.* **39**, 1–11. <https://doi.org/10.1080/0002889778507706> (1978).
- Fan, Y., Ji, X., Zhang, L. & Zhang, X. The analgesic effects of static magnetic fields. *Bioelectromagnetics* **42**, 115–127. <https://doi.org/10.1002/bem.22323> (2021).
- Zadeh-Haghighi, H. & Simon, C. Magnetic field effects in biology from the perspective of the radical pair mechanism. *J. R. Soc. Interface* **19**, 325. <https://doi.org/10.1098/rsif.2022.0325> (2022).
- Buchachenko, A. L. Magnetic field-dependent molecular and chemical processes in biochemistry, genetics and medicine. *Russ. Chem. Rev.* **83**, 1–12. <https://doi.org/10.1070/rc2014v083n01abeh004335> (2014).
- Albuquerque, W. W. C., Costa, R. M. P. B., de Salazar e Fernandes, T. & Porto, A. L. F. Evidences of the static magnetic field influence on cellular systems. *Prog. Biophys. Mol. Biol.* **121**, 16–28. <https://doi.org/10.1016/j.pbiomolbio.2016.03.003> (2016).
- McKay, J. C., Prato, F. S. & Thomas, A. W. A literature review: The effects of magnetic field exposure on blood flow and blood vessels in the microvasculature. *Bioelectromagnetics* **28**, 81–98. <https://doi.org/10.1002/bem.20284> (2007).
- Yang, J., Feng, Y., Li, Q. & Zeng, Y. Evidence of the static magnetic field effects on bone-related diseases and bone cells. *Prog. Biophys. Mol. Biol.* **177**, 168–180. <https://doi.org/10.1016/j.pbiomolbio.2022.11.006> (2023).
- Adair, R. K. Static and low-frequency magnetic field effects: Health risks and therapies. *Rep. Prog. Phys.* **63**, 415–454. <https://doi.org/10.1088/0034-4885/63/3/204> (2000).
- Bingi, V. N. & Savin, A. V. Effects of weak magnetic fields on biological systems: Physical aspects. *Phys. Usp.* **46**, 259–291. <https://doi.org/10.1070/pu2003v046n03abeh001283> (2003).
- Maffei, M. E. Magnetic field effects on plant growth, development, and evolution. *Front. Plant Sci.* **5**, 445. <https://doi.org/10.3389/fpls.2014.00445> (2014).
- Karimi, A., Moghaddam, F. G. & Valipour, M. Insights in the biology of extremely low-frequency magnetic fields exposure on human health. *Mol. Biol. Rep.* **47**, 5621–5633. <https://doi.org/10.1007/s11033-020-05563-8> (2020).
- Barnes, F. S. & Greenebaum, B. (eds) *Handbook of Biological Effects of Electromagnetic Fields—Two Volume Set* (CRC Press, 2018).
- Kim, Y. *et al.* Quantum biology: An update and perspective. *Quant. Rep.* **3**, 80–126. <https://doi.org/10.3390/quantum3010006> (2021).
- Timmel, C., Till, U., Brocklehurst, B., Mclauchlan, K. & Hore, P. Effects of weak magnetic fields on free radical recombination reactions. *Mol. Phys.* **95**, 71–89. <https://doi.org/10.1080/00268979809483134> (1998).
- Hore, P. J. & Mouritsen, H. The radical-pair mechanism of magnetoreception. *Annu. Rev. Biophys.* **45**, 299–344. <https://doi.org/10.1146/annurev-biophys-032116-094545> (2016).
- Mouritsen, H. Long-distance navigation and magnetoreception in migratory animals. *Nature* **558**, 50–59. <https://doi.org/10.1038/s41586-018-0176-1> (2018).
- Simons, W. & Dierick, M. Transcranial magnetic stimulation as a therapeutic tool in psychiatry. *World J. Biol. Psychiatry* **6**, 6–25. <https://doi.org/10.1080/15622970510029812> (2005).
- Antczak, J., Rusin, G. & Slowik, A. Transcranial magnetic stimulation as a diagnostic and therapeutic tool in various types of dementia. *J. Clin. Med.* **10**, 2875. <https://doi.org/10.3390/jcm10132875> (2021).
- Antczak, J. M. Transcranial magnetic stimulation as a diagnostic and therapeutic tool in cerebral palsy. *Adv. Psychiatry Neurol.* **30**, 203–212. <https://doi.org/10.5114/ppn.2021.110796> (2021).
- Luber, B., McClintock, S. M. & Lisanby, S. H. Applications of transcranial magnetic stimulation and magnetic seizure therapy in the study and treatment of disorders related to cerebral aging. *Dial. Clin. Neurosci.* **15**, 87–98. <https://doi.org/10.31887/dcn.2013.15.1/bluber> (2013).
- Nojima, I., Oliviero, A. & Mima, T. Transcranial static magnetic stimulation—From bench to bedside and beyond. *Neurosci. Res.* **156**, 250–255. <https://doi.org/10.1016/j.neures.2019.12.005> (2020).
- Zadeh-Haghighi, H. & Simon, C. Entangled radicals may explain lithium effects on hyperactivity. *Sci. Rep.* **11**, 9. <https://doi.org/10.1038/s41598-021-91388-9> (2021).

26. Zadeh-Haghighi, H. & Simon, C. Radical pairs can explain magnetic field and lithium effects on the circadian clock. *Sci. Rep.* **12**, 1. <https://doi.org/10.1038/s41598-021-04334-0> (2022).
27. Rishabh, R., Zadeh-Haghighi, H., Salahub, D. & Simon, C. Radical pairs may explain reactive oxygen species-mediated effects of hypomagnetic field on neurogenesis. *PLoS Comput. Biol.* **18**, e1010198. <https://doi.org/10.1371/journal.pcbi.1010198> (2022).
28. Zadeh-Haghighi, H. & Simon, C. Radical pairs may play a role in microtubule reorganization. *Sci. Rep.* **12**, 4. <https://doi.org/10.1038/s41598-022-10068-4> (2022).
29. Smith, J., Haghighi, H. Z., Salahub, D. & Simon, C. Radical pairs may play a role in xenon-induced general anesthesia. *Sci. Rep.* **11**, 1. <https://doi.org/10.1038/s41598-021-85673-w> (2021).
30. Özgün, A., Marote, A., Behie, L. A., Salgado, A. & Garipcan, B. Extremely low frequency magnetic field induces human neuronal differentiation through NMDA receptor activation. *J. Neural Transm.* **126**, 1281–1290. <https://doi.org/10.1007/s00702-019-02045-5> (2019).
31. Salunke, B. P., Umathe, S. N. & Chavan, J. G. Involvement of NMDA receptor in low-frequency magnetic field-induced anxiety in mice. *Electromagn. Biol. Med.* **33**, 312–326. <https://doi.org/10.3109/15368378.2013.839453> (2013).
32. Paoletti, P., Bellone, C. & Zhou, Q. NMDA receptor subunit diversity: Impact on receptor properties, synaptic plasticity and disease. *Nat. Rev. Neurosci.* **14**, 383–400. <https://doi.org/10.1038/nrn3504> (2013).
33. Sanz-Clemente, A., Nicoll, R. A. & Roche, K. W. Diversity in NMDA receptor composition. *Neuroscientist* **19**, 62–75. <https://doi.org/10.1177/1073858411435129> (2012).
34. Paoletti, P. & Neyton, J. NMDA receptor subunits: Function and pharmacology. *Curr. Opin. Pharmacol.* **7**, 39–47. <https://doi.org/10.1016/j.coph.2006.08.011> (2007).
35. Monyer, H. *et al.* Heteromeric NMDA receptors: Molecular and functional distinction of subtypes. *Science* **256**, 1217–1221. <https://doi.org/10.1126/science.256.5060.1217> (1992).
36. Furukawa, H., Singh, S. K., Mancusso, R. & Gouaux, E. Subunit arrangement and function in NMDA receptors. *Nature* **438**, 185–192. <https://doi.org/10.1038/nature04089> (2005).
37. Hansen, K. B., Yi, F., Perszyk, R. E., Menniti, F. S. & Traynelis, S. F. NMDA receptors in the central nervous system. In *Methods in Molecular Biology* (eds Hansen, K. B. *et al.*) 1–80 (Springer, 2017).
38. Liu, J., Chang, L., Song, Y., Li, H. & Wu, Y. The role of NMDA receptors in Alzheimer's disease. *Front. Neurosci.* **13**, 43. <https://doi.org/10.3389/fnins.2019.00043> (2019).
39. Nakazawa, K. & Sapkota, K. The origin of NMDA receptor hypofunction in schizophrenia. *Pharmacol. Therap.* **205**, 107426. <https://doi.org/10.1016/j.pharmthera.2019.107426> (2020).
40. Zhou, Q. & Sheng, M. NMDA receptors in nervous system diseases. *Neuropharmacology* **74**, 69–75. <https://doi.org/10.1016/j.neuropharm.2013.03.030> (2013).
41. Hirai, T. & Yoneda, Y. Functional alterations in immature cultured rat hippocampal neurons after sustained exposure to static magnetic fields. *J. Neurosci. Res.* **75**, 230–240. <https://doi.org/10.1002/jnr.10819> (2003).
42. Hirai, T. *et al.* Counteraction by repetitive daily exposure to static magnetism against sustained blockade of n-methyl-d-aspartate receptor channels in cultured rat hippocampal neurons. *J. Neurosci. Res.* **80**, 491–500. <https://doi.org/10.1002/jnr.20497> (2005).
43. Qiang, M. & Ticku, M. K. Role of AP-1 in ethanol-induced n-methyl-d-aspartate receptor 2b subunit gene up-regulation in mouse cortical neurons. *J. Neurochem.* **95**, 1332–1341. <https://doi.org/10.1111/j.1471-4159.2005.03464.x> (2005).
44. Prybylowski, K. *et al.* Relationship between availability of NMDA receptor subunits and their expression at the synapse. *J. Neurosci.* **22**, 8902–8910. <https://doi.org/10.1523/jneurosci.22-20-08902.2002> (2002).
45. Gupta, S. *et al.* Selective interaction of JNK protein kinase isoforms with transcription factors. *EMBO J.* **15**, 2760–2770. <https://doi.org/10.1002/j.1460-2075.1996.tb00636.x> (1996).
46. Kallunki, T., Deng, T., Hibi, M. & Karin, M. c-jun can recruit JNK to phosphorylate dimerization partners via specific docking interactions. *Cell* **87**, 929–939. [https://doi.org/10.1016/s0092-8674\(00\)81999-6](https://doi.org/10.1016/s0092-8674(00)81999-6) (1996).
47. Markov, M. & Pilla, A. Weak static magnetic field modulation of myosin phosphorylation in a cell-free preparation: Calcium dependence. *Bioelectrochem. Bioenergy* **43**, 233–238. [https://doi.org/10.1016/s0302-4598\(96\)02226-x](https://doi.org/10.1016/s0302-4598(96)02226-x) (1997).
48. Engström, S., Markov, M. S., McLean, M. J., Holcomb, R. R. & Markov, J. M. Effects of non-uniform static magnetic fields on the rate of myosin phosphorylation. *Bioelectromagnetics* **23**, 475–479. <https://doi.org/10.1002/bem.10035> (2002).
49. Buchachenko, A. L., Kouznetsov, D. A., Orlova, M. A. & Markarian, A. A. Magnetic isotope effect of magnesium in phosphoglycerate kinase phosphorylation. *Proc. Natl. Acad. Sci.* **102**, 10793–10796. <https://doi.org/10.1073/pnas.0504876102> (2005).
50. Chen, B.-S. & Roche, K. W. Regulation of NMDA receptors by phosphorylation. *Neuropharmacology* **53**, 362–368. <https://doi.org/10.1016/j.neuropharm.2007.05.018> (2007).
51. Wang, J. Q. *et al.* Roles of subunit phosphorylation in regulating glutamate receptor function. *Eur. J. Pharmacol.* **728**, 183–187. <https://doi.org/10.1016/j.ejphar.2013.11.019> (2014).
52. Buchachenko, A. L. Magnetic control of enzymatic phosphorylation. *J. Phys. Chem. Biophys.* **2**, 142. <https://doi.org/10.4172/2161-0398.1000142> (2014).
53. Efimova, O. & Hore, P. Role of exchange and dipolar interactions in the radical pair model of the avian magnetic compass. *Biophys. J.* **94**, 1565–1574. <https://doi.org/10.1529/biophysj.107.119362> (2008).
54. Hore, P. Upper bound on the biological effects of 50/60 Hz magnetic fields mediated by radical pairs. *eLife* **8**, 44179. <https://doi.org/10.7554/eLife.44179> (2019).
55. Green, S. P., Jones, C. & Stasch, A. Stable magnesium(I) compounds with Mg–Mg bonds. *Science* **318**, 1754–1757. <https://doi.org/10.1126/science.1150856> (2007).
56. Buchachenko, A. L. *et al.* Dependence of mitochondrial ATP synthesis on the nuclear magnetic moment of magnesium ions. *Dokl. Biochem. Biophys.* **396**, 197–199. <https://doi.org/10.1023/b:dobi.0000033528.69032.9b> (2004).
57. Buchachenko, A. L., Kouznetsov, D. A., Arkhangel'sky, S. E., Orlova, M. A. & Markarian, A. A. Spin biochemistry: Intramitochondrial nucleotide phosphorylation is a magnesium nuclear spin controlled process. *Mitochondrion* **5**, 67–69. <https://doi.org/10.1016/j.mito.2004.10.001> (2005).
58. Buchachenko, A. L., Lukzen, N. N. & Boiden Pedersen, J. On the magnetic field and isotope effects in enzymatic phosphorylation. *Chem. Phys. Lett.* **434**, 139–143. <https://doi.org/10.1016/j.cplett.2006.12.019> (2007).
59. Buchachenko, A. L. & Kouznetsov, D. A. Magnetic field affects enzymatic ATP synthesis. *J. Am. Chem. Soc.* **130**, 12868–12869. <https://doi.org/10.1021/ja804819k> (2008).
60. Buchachenko, A. L., Kouznetsov, D. A., Breslavskaya, N. N. & Orlova, M. A. Magnesium isotope effects in enzymatic phosphorylation. *J. Phys. Chem. B* **112**, 2548–2556. <https://doi.org/10.1021/jp710989d> (2008).
61. Zadeh-Haghighi, H. & Simon, C. Magnetic isotope effects: A potential testing ground for quantum biology. *Front. Physiol.* **14**, 479. <https://doi.org/10.3389/fphys.2023.1338479> (2023).
62. Letuta, U. G., Avdeeva, E. I. & Berdinsky, V. L. Magnetic field effects in bacteria *E. coli* in the presence of Mg isotopes. *Russ. Chem. Bull.* **63**, 1102–1106. <https://doi.org/10.1007/s11172-014-0555-1> (2014).
63. Letuta, U. G. & Berdinskiy, V. L. Effects of the magnetic field and zinc isotopes on the colony forming ability and elemental composition of *E. coli* bacterial cells. *Russ. Chem. Bull.* **67**, 1732–1737. <https://doi.org/10.1007/s11172-018-2283-4> (2018).
64. Koltover, V. K., Labyntseva, R. D., Karandashev, V. K. & Kosterin, S. O. Magnetic isotope of magnesium accelerates ATP hydrolysis catalyzed by myosin. *Biophysics* **61**, 200–206. <https://doi.org/10.1134/s0006350916020068> (2016).

65. Letuta, U. G., Letuta, S. N. & Berdinskiy, V. L. The influence of low magnetic fields and magnesium isotopes on *E. coli* bacteria. *Biophysics* **62**, 935–941. <https://doi.org/10.1134/s0006350917060112> (2017).
66. Koltover, V. K. *et al.* Magnetic-isotope effect of magnesium in the living cell. *Dokl. Biochem. Biophys.* **442**, 12–14. <https://doi.org/10.1134/s1607672912010048> (2012).
67. Crotty, D. *et al.* Reexamination of magnetic isotope and field effects on adenosine triphosphate production by creatine kinase. *Proc. Natl. Acad. Sci.* **109**, 1437–1442. <https://doi.org/10.1073/pnas.1117840108> (2011).
68. Hore, P. J. Are biochemical reactions affected by weak magnetic fields? *Proc. Natl. Acad. Sci.* **109**, 1357–1358. <https://doi.org/10.1073/pnas.1120531109> (2012).
69. Lacy-hulbert, A., Metcalfe, J. C. & Hesketh, R. Biological responses to electromagnetic fields. *FASEB J.* **12**, 395–420. <https://doi.org/10.1096/fasebj.12.6.395> (1998).
70. <https://doi.org/10.1126/science.acx9770> (2021).
71. Buchachenko, A. Why magnetic and electromagnetic effects in biology are irreproducible and contradictory? *Bioelectromagnetics* **37**, 1–13. <https://doi.org/10.1002/bem.21947> (2015).
72. Kattnig, D. R. *et al.* Chemical amplification of magnetic field effects relevant to avian magnetoreception. *Nat. Chem.* **8**, 384–391. <https://doi.org/10.1038/nchem.2447> (2016).
73. Kattnig, D. R. & Hore, P. J. The sensitivity of a radical pair compass magnetoreceptor can be significantly amplified by radical scavengers. *Sci. Rep.* **7**, 7. <https://doi.org/10.1038/s41598-017-09914-7> (2017).
74. Player, T. C., Baxter, E. D. A., Allatt, S. & Hore, P. J. Amplification of weak magnetic field effects on oscillating reactions. *Sci. Rep.* **11**, 8. <https://doi.org/10.1038/s41598-021-88871-8> (2021).
75. Binhi, V. N. Statistical amplification of the effects of weak magnetic fields in cellular translation. *Cells* **12**, 724. <https://doi.org/10.3390/cells12050724> (2023).
76. Forbes, M. D. E. *et al.* On the electron spin polarization observed in TREPR experiments involving hydroxyl and sulfate radicals. *Mol. Phys.* **105**, 2127–2136. <https://doi.org/10.1080/00268970701663768> (2007).
77. Heo, J. & Campbell, S. L. Ras regulation by reactive oxygen and nitrogen species. *Biochemistry* **45**, 2200–2210. <https://doi.org/10.1021/bi051872m> (2006).
78. Liming, F. G. Free radicals formed in aliphatic polyamino acids by exposure to hydrogen atoms. *Radiat. Res.* **39**, 252. <https://doi.org/10.2307/3572665> (1969).
79. Neese, F. The ORCA program system. *WIREs Comput. Mol. Sci.* **2**, 73–78. <https://doi.org/10.1002/wcms.81> (2012).

Acknowledgements

The authors would like to thank Dennis Salahub for helpful feedback. This work was supported by the Natural Sciences and Engineering Research Council (NSERC) and the National Research Council (NRC) of Canada.

Author contributions

H.Z.-H. and C.S. conceived the project; P.S.N. conducted the investigation and performed the modelling and calculations with help from H.Z.-H. and C.S.; P.S.N. wrote the paper with feedback from H.Z.-H. and C.S.

Competing interests

The authors declare no competing interests.

Additional information

Supplementary Information The online version contains supplementary material available at <https://doi.org/10.1038/s41598-024-54343-y>.

Correspondence and requests for materials should be addressed to P.S.N., H.Z.-H. or C.S.

Reprints and permissions information is available at www.nature.com/reprints.

Publisher's note Springer Nature remains neutral with regard to jurisdictional claims in published maps and institutional affiliations.



Open Access This article is licensed under a Creative Commons Attribution 4.0 International License, which permits use, sharing, adaptation, distribution and reproduction in any medium or format, as long as you give appropriate credit to the original author(s) and the source, provide a link to the Creative Commons licence, and indicate if changes were made. The images or other third party material in this article are included in the article's Creative Commons licence, unless indicated otherwise in a credit line to the material. If material is not included in the article's Creative Commons licence and your intended use is not permitted by statutory regulation or exceeds the permitted use, you will need to obtain permission directly from the copyright holder. To view a copy of this licence, visit <http://creativecommons.org/licenses/by/4.0/>.

© The Author(s) 2024